Available online at www.sciencedirect.com
ScienceDirect
Journal of Magnetic Resonance 187 (2007) 88–96
JMR Journal of Magnetic Resonance
www.elsevier.com/locate/jmr

Determination of the ^{19}F NMR chemical shielding tensor and crystal structure of 5-fluoro-DL-tryptophan

Xingang Zhao [a], Jeffrey S. DeVries [a], Robert McDonald [b], Brian D. Sykes [a,*]

[a] Department of Biochemistry, University of Alberta, 419 Medical Sciences Building, Edmonton, Alta., Canada T6G 2H7
[b] Department of Chemistry, University of Alberta, Edmonton, Alta., Canada T6G 2H7

Received 22 December 2006; revised 13 March 2007
Available online 14 April 2007

Abstract

5-Fluoro-DL-tryptophan (5F-Trp) is a very sensitive probe used to investigate orientation and dynamics of biomacromolecules at the *in situ* level. In order to establish a ^{19}F NMR strategy, the crystal structure and ^{19}F chemical shielding tensor of 5F-Trp are reported. A novel approach was developed to use F–F homonuclear dipole–dipole coupling information to analyze single-crystal NMR data without determining crystal orientations. The measured values for the principal components of the shielding tensor are $\sigma_{11} = 0.9$, $\sigma_{22} = -63.3$, and $\sigma_{33} = -82.9$ ppm relative to TFA in D_2O. The principal axes of the shielding tensors coincide with the indole ring symmetry, which makes it a straightforward and powerful tool to monitor protein alignment in oriented environments. Hartree–Fock (HF) and density functional theory (DFT) calculations of the chemical shielding tensors are also reported.

Keywords: Fluorine-19 NMR; Chemical shift tensor; Homonuclear dipole–dipole interactions; Biomacromolecule orientation and dynamics

1. Introduction

X-ray crystallography and liquid-state high resolution NMR methods have developed rapidly and have become the most widely used tools in peptide and protein structural biology. Recently, solid-state NMR spectroscopy has advanced remarkably, evolving from a tool for small molecules into a powerful approach to provide atomic-level structural constraints on complex biomacromolecules and supramolecular structures. Many promising results have been recently obtained for membrane proteins [1–3] and amyloid fibrils [4].

^{19}F NMR has been of interest for many years as a versatile tool for the investigation of biological molecules because it has several advantages. First of all, 100% naturally abundant ^{19}F nuclei possess the highest gyromagnetic ratio except for ^{1}H and ^{3}H, producing high NMR sensitivity. Unlike ^{1}H, ^{19}F NMR has a large chemical shift range, making ^{19}F chemical shifts a useful probe of the local environment. ^{19}F NMR also benefits from the lack of biological background and becomes a selective alternative to more conventional isotopes (^{13}C and ^{15}N). In fact, only six distinct natural compounds were found to contain ^{19}F atoms to date [5]. Consequently, ^{19}F NMR has been widely used to survey dynamic and structural information in macromolecules [6–9] in the liquid state. Recently, Ulrich and coworkers have also successfully applied solid-state ^{19}F NMR methods to study biomembranes [10].

The research in our lab has focused on the elucidation of the structural details of peptides and proteins in cardiac and skeletal muscle to help us understand the biological mechanism of muscle regulation in the human heart and provide useful information to help cure cardiovascular disease, which is the leading cause of death among men and women in North America [11]. Previously, much structural and dynamic information on important regulatory proteins, such as the troponin subunits, have been obtained on proteins extracted from muscle and studied in solution [12–14]. However, striated muscle is an elegant supramolecular

* Corresponding author. Fax: +1 780 492 0886.
E-mail address: brian.sykes@ualberta.ca (B.D. Sykes).

1090-7807/$ - see front matter © 2007 Elsevier Inc. All rights reserved.
doi:10.1016/j.jmr.2007.03.022

system and some molecular details underlying contraction can not be unraveled at the level of *in vitro* structures. Solid-state ^{19}F NMR can be an effective technique for *in situ* investigations. One or a few well selected fluorine labels in a macromolecule can provide valuable information such as its alignment relative to the specific frame and its interaction with the environment, so that high resolution structures and dynamic changes can be connected with physiological and functional measurements. It should be noted that results obtained using ^{19}F labeling methods are useful only if they render minimal perturbation to the biological system. Recently used successful fluorine containing analogs include 5-fluorotryptophan, 6-fluorotryptophan, 4-fluorophenylglycine, and CF_3-phenylglycine [10]. Single 5F-Trp residues have been incorporated into cardiac troponin-C proteins without generating significant structural changes [15].

Before we begin to use ^{19}F NMR on biomacromolecules, we need to confidently understand the fundamental NMR properties and make sure that the solid-state ^{19}F NMR theory and spectra can be adequately elucidated in small molecules. Tryptophan is an essential amino acid and often plays an important role in biological functions. For example, the dipole moment of its indole ring can act as an ion channel modulator [16–18]. Often, few tryptophan residues occur naturally in proteins so they can be exclusively studied. Both Raman and fluorescence spectroscopy of tryptophan have been used to monitor the structural and dynamic information in proteins [19–22]. The ^{19}F-substituent 5F-Trp can be a powerful probe for monitoring the local conformation and dynamics at the *in situ* level and it has been proven to be biocompatible with its cognate amino acid in many cases [10,15,23–25]. However, the fundamental ^{19}F chemical shielding tensor information in 5F-Trp has not yet been fully elucidated. In this work we have therefore undertaken single-crystal NMR methods to obtain all six independent elements of the ^{19}F chemical shielding tensor. These are useful to test methods and theories and are prerequisite references for future protein *in situ* studies. The crystal structure of 5F-Trp has not yet been reported, so it was determined in this work. A new goniometer ^{19}F NMR probe (Fig. 1) combining a worm gear [26] and a split radio-frequency coil [27] was developed to perform single-crystal NMR investigations. This design allows us not only to be able to mount the small crystal easily and accurately in three axes perpendicular to the main magnetic field (B_0), but also improves the precision of the stepwise rotation.

2. Methods

5-Fluoro-DL-tryptophan was purchased from Sigma–Aldrich Canada (Oakville, ON) and single crystals were grown from ethanol solution by slow evaporation at room temperature. A single-crystal measuring $0.56 \times 0.43 \times 0.26$ mm was used in the X-ray crystallography study. Unit cell determination and data collection were performed on a non-specific orientation with a Bruker SMART 1000CCD PLATFORM diffractometer system. All intensity measurements were performed using MoKα radiation ($\lambda = 0.71073$ Å) with a graphite crystal incident beam monochromator. Two thousand and forty-six independent reflections were collected at -80 °C using ω scans (0.3°, 10 s exposures). The crystal structure was solved by *SHELXS*–86 direct methods [28]. Refinement of atomic parameters was performed with full-matrix least-squares on F^2 (*SHELXL*–93) [29] giving final R indices of $R_1(F) = 0.0463$ (for 1765 data with $I \geqslant 2\sigma(I)$) and $wR_2(F^2) = 0.1463$ (for all 2046 unique reflections). The hydrogen atoms attached to carbons were generated in idealized positions based on the sp2 or sp3 hybridization of the parent carbon atoms. The hydrogen atoms on N1 and N2 were located by using a difference Fourier map, which confirmed that three hydrogen atoms were bonded to N2, and that none were within bonding distance of the oxygen atoms. These hydrogen atoms were then refined in idealized positions, assuming an sp2 hybridization of

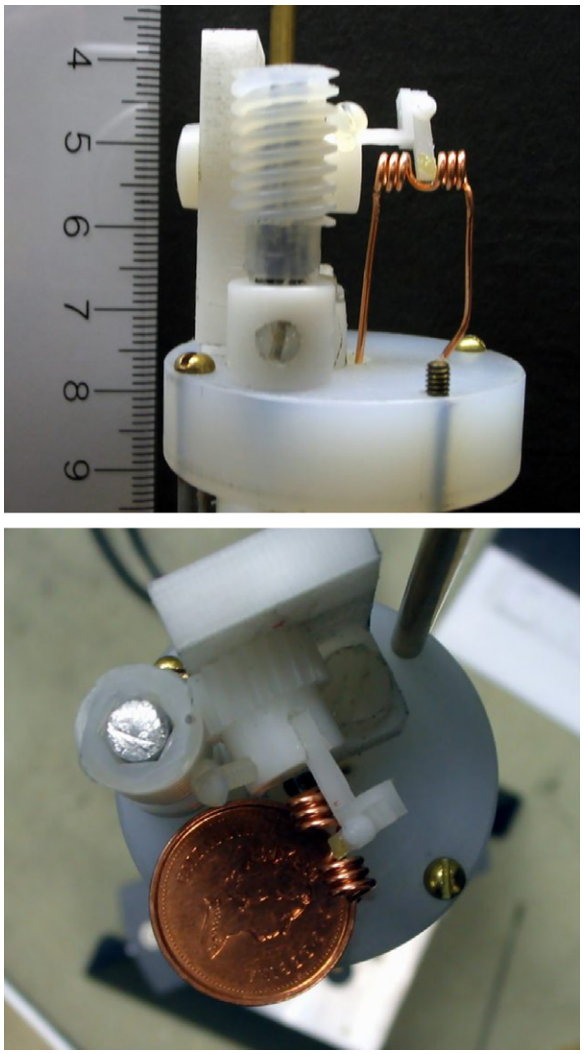

Fig. 1. Goniometer portion of the single-crystal NMR probe. All the gears and crystal holder parts are made from fluorine free acetal.

N1 and an sp3 hybridization of N2. For the hydrogen-bonded interactions, we searched nearest-neighbor interactions that yielded N–H···O non-bonded distances of $\leqslant$2.2 Å, or, ignoring the idealized N–H hydrogen positions, N···O non-bonded distances of $\leqslant$3.0 Å. No notable N–H···N or N–H···F interactions were found.

Resolve-Al™ Gd (12 mg) was ordered from Adrich and crystallized together with 5F-Trp (180 mg) to reduce the T_1. A Gd doped single-crystal with appropriate dimensions ($3.8 \times 2.1 \times 0.26$ mm) was used for the ^{19}F NMR measurements. Its crystal structure was unchanged as verified by X-ray diffraction. T_1 value was decreased to 44 from 234 s in non-doped crystals. All the NMR spectra were performed on a Varian INOVA UNITY-600 spectrometer using a home built narrow bore probe, which was discussed elsewhere [30]. Fig. 1 shows the picture of the goniometer added to this probe for single-crystal NMR investigations. The acetal worm gear and its adaptor were ordered from Sterling Instrument, New York. All other parts were machined to a very high precision at the pharmacology department machine shop at the University of Alberta. The sample was glued onto the cuboid shaped holder and was transferred easily between each of three orientations. The split-coil design was adapted from Hauser et al [27]. Although a split coil can introduce compromises, the performance of this probe was gratifying. ^{19}F NMR spectra were recorded for 20 orientations (9° rotation between each position) in each of three orthogonal rotations with proton decoupling. The DEPTH sequence was employed to suppress background [31]. The ^{19}F 90° pulse was 3.2 μs and 32 acquisitions were accumulated for each orientation, with a recycle delay of 100 s. The γB_1 for ^{1}H decoupling was 63.5 kHz. The ^{19}F NMR signal of sodium trifluoroacetate (TFA) in D_2O was used as a chemical shift reference, where TFA is at -76.5 ppm relative to $CFCl_3$ at 0 ppm.

There are two chemically equivalent but magnetically distinct molecules in the 5F-Trp unit cell. This generates ambiguities in assigning a particular signal to a given fluorine atom. Six unique orientations out of all possible rotations provide three constraints to solve this problem. The chemical shifts and dipolar coupling values at 0° position in x rotation should be identical with that at 90° position in z rotation: $x(0°) = z(90°)$ because the angles between the crystal and the external field are the same. Similarly we have $y(0°) = z(0°)$ and $x(90°) = y(90°)$. These constraints give us enough information to assign each magnetically distinct fluorine atom.

The conventional single-crystal NMR data processing method has been well discussed [41] and will not be repeated here. Rotation plots of the resolved splitting from the single F–F homonuclear dipole coupling in the single-crystal NMR spectra can be fit with the theoretically calculated values to obtain the three Euler angles $(\alpha_X, \beta_X, \gamma_X)$ relating the crystal holder frame to the crystallographic frame. We start with the crystallographic frame in which the vector of dipolar coupled F–F ($\vec{V}_{XF}$) can be calculated from X-ray diffraction data. The transformation from crystallographic frame (**XF**) to crystal holder frame (**CH**) can be accomplished by rotation matrix $R_X(\alpha_X, \beta_X, \gamma_X)$:

$$R_X(\alpha_X,\beta_X,\gamma_X) = \begin{pmatrix} \cos\alpha_X & -\sin\alpha_X & 0 \\ \sin\alpha_X & \cos\alpha_X & 0 \\ 0 & 0 & 1 \end{pmatrix} \times \begin{pmatrix} \cos\beta_X & 0 & \sin\beta_X \\ 0 & 1 & 0 \\ -\sin\beta_X & 0 & \cos\beta_X \end{pmatrix} \times \begin{pmatrix} \cos\gamma_X & -\sin\gamma_X & 0 \\ \sin\gamma_X & \cos\gamma_X & 0 \\ 0 & 0 & 1 \end{pmatrix}$$

Transformation from crystal holder frame (**CH**) to goniometer frame (**GF**) is accomplished by $R_G = R_Z(\alpha_G)\, R_Y(\beta_G)\, R_Z(\gamma_G)$:

$$R_G = \begin{pmatrix} 1 & 0 & 0 \\ 0 & 1 & 0 \\ 0 & 0 & 1 \end{pmatrix} \quad \text{for } x \text{ rotation;}$$

$$R_G = \begin{pmatrix} 0 & 0 & -1 \\ 0 & 1 & 0 \\ 1 & 0 & 0 \end{pmatrix} \quad \text{for } y \text{ rotation;}$$

and

$$R_G = \begin{pmatrix} 0 & 0 & -1 \\ 1 & 0 & 0 \\ 0 & -1 & 0 \end{pmatrix} \quad \text{for } z \text{ rotation.}$$

Finally, because the sample is rotated in the goniometer anti-clockwise by an angle θ, transformation from the goniometer frame (**GF**) to lab frame (**LF**) is accomplished by

$$R_L = \begin{pmatrix} \sin\theta & \cos\theta & 0 \\ 0 & 0 & 1 \\ \cos\theta & -\sin\theta & 0 \end{pmatrix}$$

The overall transformation from XF to LF is the product: $R = R_L R_G R_X$. The vector of dipolar coupled F–F in the lab frame ($\vec{V}_{LF}$) can be obtained by:

$$\vec{V}_{LF} = R_L R_G R_X \cdot \vec{V}_{XF}$$

After we find $\vec{V}_{LF}$, homonuclear F–F dipolar coupling can be calculated from:

$$\Delta_{FF} = \tfrac{d}{2}(3\cos^2\phi - 1)$$

d is a constant related to the ^{19}F gyromagnetic ratio and the distance between two fluorine atoms, which is equal to 1.1×10^4 Hz when the fluorine atoms are separated by 3.08 Å. ϕ is the angle between $\vec{V}_{LF}$ and magnetic field $\vec{B}_0$ so we have

$$\cos\phi = \vec{V}_{LF} \cdot \vec{B}_0$$

and the overall equation for calculating homonuclear F–F dipolar coupling is:

$$\Delta_{FF} = \frac{d}{2}\left[3(\vec{V}_{LF}\cdot\vec{B}_0)^2 - 1\right]$$

Therefore the three Euler angles $(\alpha_X, \beta_X, \gamma_X)$ relating the crystal holder frame to the crystallographic frame can be obtained from the best fit of the dipolar splitting experimental data by least squares methods.

Hartree–Fock (HF) and density functional theory (DFT) calculations were performed using the Gaussian 03 program package [32] on a 25 node Linux cluster. The geometries for 5F-Trp and the reference compound TFA were optimized at both HF and B3LYP hybrid functional methods [33,34] with the 6-31G++(d,p) basis set [35]. ^{19}F NMR shielding tensors were calculated using the gauge-independent atomic orbital (GIAO) method [36–38].

3. Results

X-ray crystal data are given in Table 1 and the atomic position parameters listed in Table 2. The 5-Fluoro-DL-tryptophan crystals are monoclinic ($a = 13.847$, $b = 6.8728$, $c = 10.7603$ Å, $\beta = 103.184°$; $Z = 4$) and belong to space group $P2_1/c$. This structure is different from 5-fluoro-L-tryptophan, which contains two molecules in each unit cell and belongs to $P2_1$ space group [39]. As with most amino acids, 5F-Trp exists in the zwitterionic form in crystals. The inversion center yields a twofold degeneration from the NMR point of view and, therefore, each unit cell contains two magnetically nonequivalent molecules. Similar to the parent molecule—DL-tryptophan [40], the protonated amino group is the donor of three hydrogen bonds and plays an important role in crystal packing. The N2–H2B···O1 bond connects two molecules and the other two hydrogen bonds between amino group and carboxy oxygen atoms link the system in a and c directions. Meanwhile, the indole nitrogen forms a N1–H1···O2 hydrogen bond stabilizing the network in b direction. All the major hydrogen bond interactions are illustrated in Fig. 2. Overall, the crystal structure is more compact than DL-tryptophan.

The elements of the ^{19}F chemical shielding tensor in the principal axis frame and its orientation in the crystallographic reference frame were determined using the traditional single-crystal NMR technique [41]. Fig. 3 shows all the single-crystal NMR spectra in three orthogonal rotations. As mentioned above, the space group of 5F-Trp is $P2_1/c$ with four molecules per unit cell. The inversion center generates a two-fold degeneration in NMR so that two distinguishable ^{19}F signals are observed. From the crystal structure, it can be noticed that a single F–F intermolecular contact dominates the F–F dipole coupling. The distance

Table 1
Crystallographic data

Formula	$C_{11}H_{11}FN_2O_2$
Formula weight	222.22
Crystal dimensions (mm)	$0.56 \times 0.43 \times 0.26$
Crystal system	Monoclinic
Space group	$P2_1/c$ (No. 14)
Unit cell parameters[a]	
a (Å)	13.847 (2)
b (Å)	6.8728 (12)
c (Å)	10.7603 (18)
β (deg)	103.184 (2)
V (Å^3)	997.0 (3)
Z	4
ρ_{calcd} (g cm^{-3})	1.480
μ (mm^{-1})	0.116

[a] Obtained from least-squares refinement of 3972 reflections with $6.04° < 2\theta < 52.74°$.

Table 2
Atomic coordinates and equivalent isotropic displacement parameters

Atom	x	y	z	U_{eq}, Å^2
F	0.02413(10)	0.1251(2)	0.12191(12)	0.0543(4)*
O1	0.47617(9)	0.28343(17)	0.09977(10)	0.0250(3)*
O2	0.38210(9)	0.01761(17)	0.07104(11)	0.0279(3)*
N1	0.24832(12)	0.7061(2)	−0.0074(2)	0.0460(5)*
N2	0.48213(10)	0.3081(2)	−0.14593(12)	0.0226(3)*
C1	0.29253(14)	0.6095(3)	−0.0902(2)	0.0395(5)*
C2	0.26376(12)	0.4190(3)	−0.09989(17)	0.0282(4)*
C3	0.19602(12)	0.3972(3)	−0.01728(16)	0.0259(4)*
C4	0.13964(12)	0.2403(3)	0.01023(16)	0.0270(4)*
C5	0.08039(14)	0.2747(3)	0.09408(18)	0.0352(5)*
C6	0.07320(15)	0.4524(4)	0.15188(19)	0.0426(5)*
C7	0.12728(15)	0.6078(3)	0.1254(2)	0.0442(5)*
C8	0.18836(13)	0.5787(3)	0.03997(19)	0.0347(4)*
C9	0.29861(12)	0.2595(3)	−0.17393(16)	0.0296(4)*
C10	0.40351(11)	0.1823(2)	−0.11379(14)	0.0219(4)*
C11	0.42165(11)	0.1601(2)	0.03110(15)	0.0203(3)*

Anisotropically-refined atoms are marked with an asterisk (*). The form of the anisotropic displacement parameter is: $\exp[-2\pi^2(h^2a^{*2}U_{11} + k^2b^{*2}U_{22} + l^2c^{*2}U_{33} + 2klb^*c^*U_{23} + 2hla^*c^*U_{13} + 2hka^*b^*U_{12})]$.

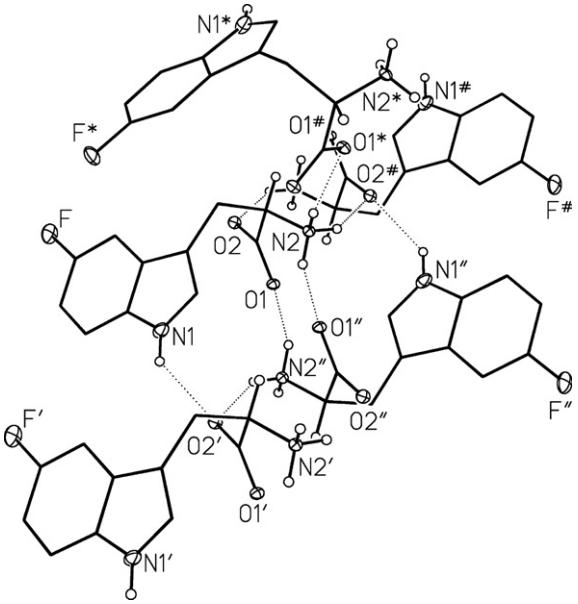

Fig. 2. Illustration of hydrogen-bonded interactions between adjacent 5- fluoro-DL-tryptophan molecules in the crystal lattice. Primed atoms are related to unprimed ones via the symmetry operation $(x, 1 + y, z)$. Double-primed atoms are related to unprimed ones via the symmetry operation $(1 - x, 1 - y, \bar{z})$. Starred atoms are related to unprimed ones via the symmetry operation $(x, 1/2^{-}y, -1/2 + z)$. Atoms marked with an octothorpe (#) are related to unprimed ones via the symmetry operation $(1 - x, \bar{y}, \bar{z})$.

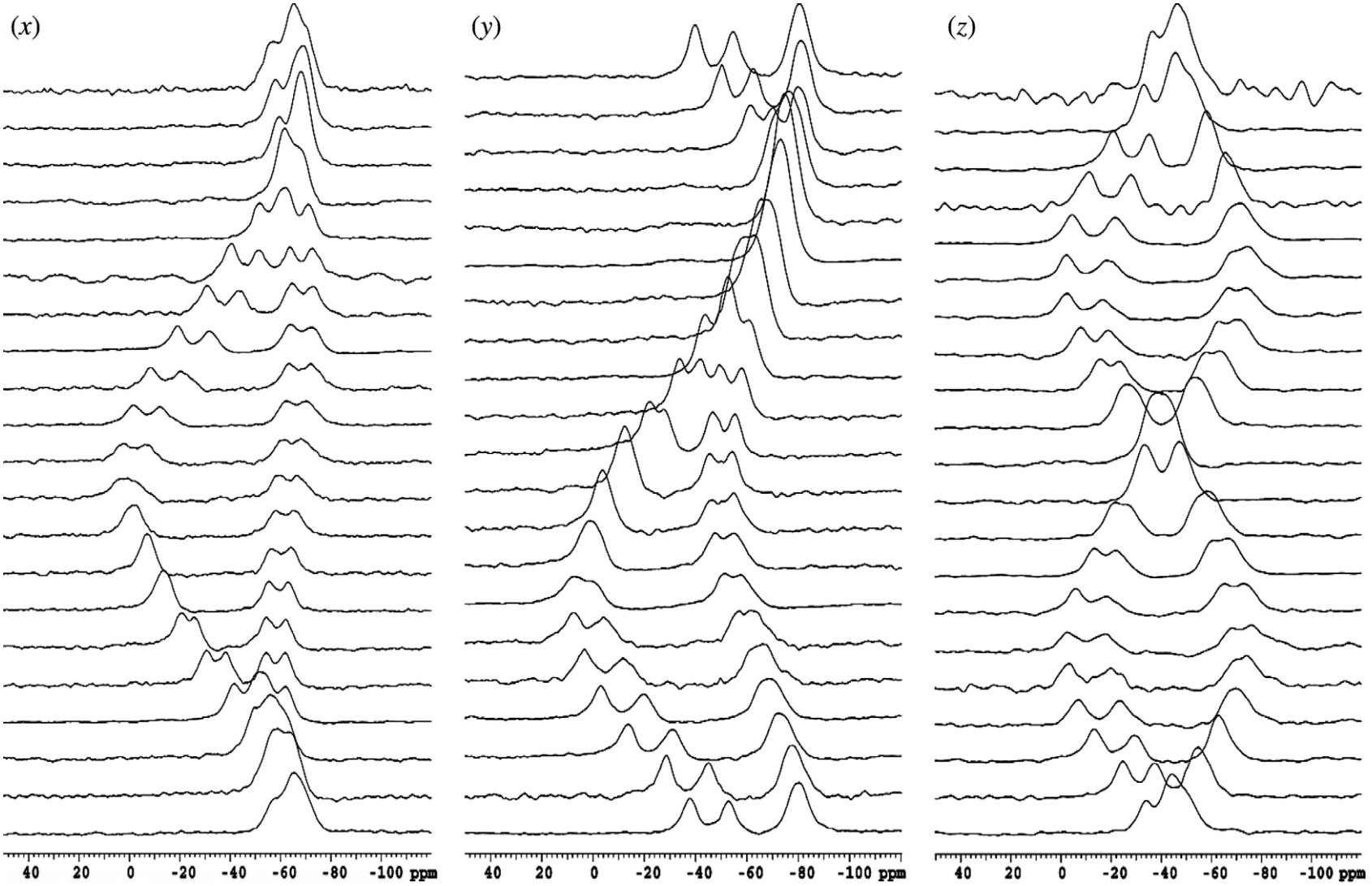

Fig. 3. The single-crystal NMR spectra taken from rotations about the x, y, and z axis in the crystal holder frame. The interval between each orientation is 9°. Chemical shifts were referenced to TFA.

between these two fluorine atoms is 3.08 Å, therefore, each ^{19}F NMR signal is present as a doublet with up to 11 kHz homonuclear dipolar splitting depending on orientation. The next nearest F–F contact is 4.56 Å. It will have much less homonuclear dipolar splitting and only impacts the line widths of ^{19}F NMR spectra. In order to separate chemical shifts and dipolar splitting values, the ^{19}F NMR spectra are deconvolved with a pair of doublets. Each doublet is related to each individual magnetically nonequivalent fluorine atom. Chemical shift values are calculated by the average frequencies of the doublets and dipolar splittings are equal to the frequency differences. Fig. 4 gives three rotation plots for ^{19}F chemical shift values retrieved from the three mutually orthogonal rotation axes. Chemical shielding tensor principal values and orientations were obtained by least-squares refinement of the rotation plots and are listed

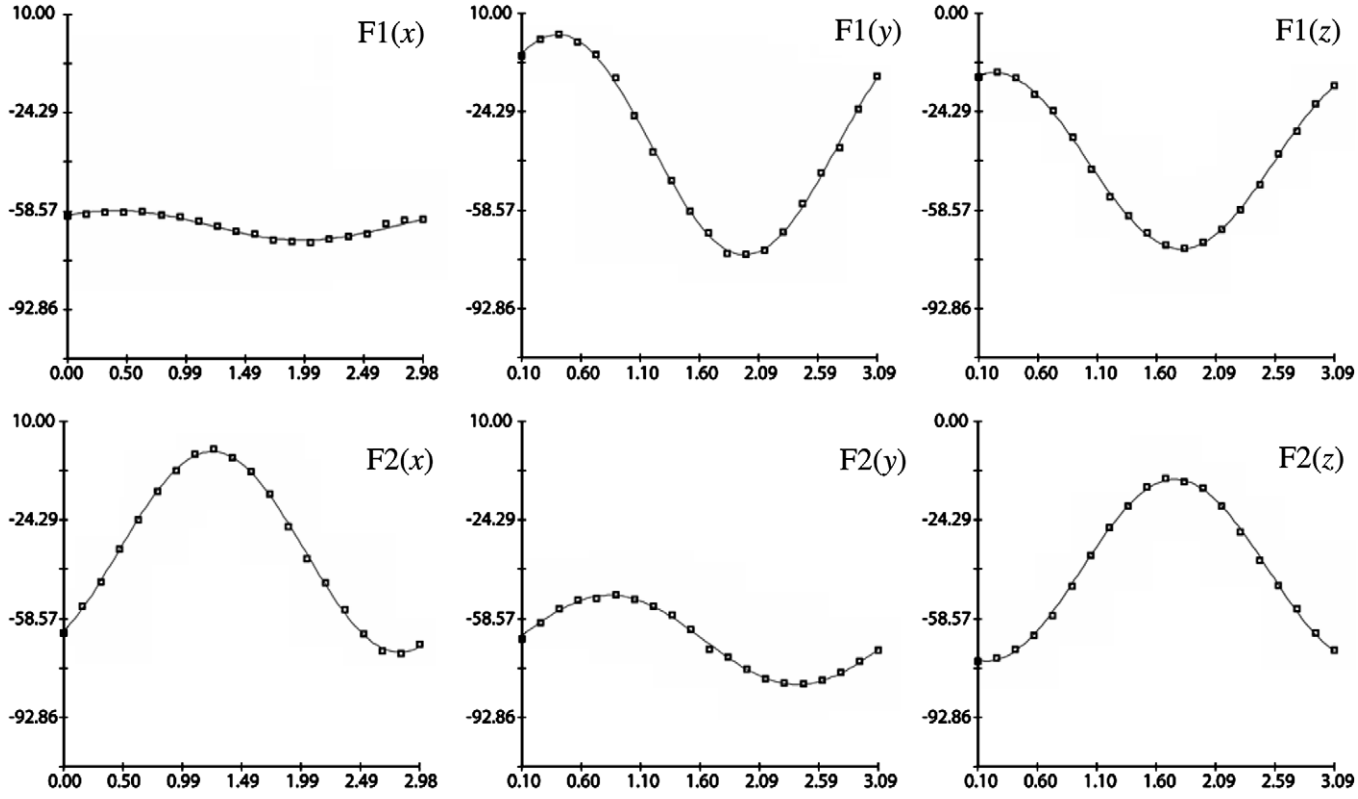

Fig. 4. All the ^{19}F NMR spectra in Fig. 3 are deconvolved with a pair of doublets and provide us with separated chemical shift and dipolar coupling values. These three rotation plots only show the observed ^{19}F chemical shifts. Two magnetically nonequivalent ^{19}F atoms were separated. Rectangle shape points are experimental values and solid lines are theoretical curves computed by a least-squares analysis. The vertical axes in these plots are chemical shifts (ppm) referenced to TFA and the horizontal axes are the rotation angles (radian) of the goniometer.

Table 3
Experimentally and theoretically calculated ^{19}F chemical shift tensor principal values and direction cosines of the principal axes in the crystallographic (a,b,c) and the local molecular frame (x,y,z)

	ppm	*a*	*b*	*C*	*x*	*y*	*z*
F1							
σ_{11}	0.1	0.2222	−0.9094	0.3517	0.9982	0.0017	− 0.0594
σ_{22}	−62.3	0.6526	0.4067	0.6393	0.0240	0.9997	− 0.0003
σ_{33}	−83.5	0.7244	−0.0874	−0.6838	0.0595	−0.0239	0.9979
F2							
σ_{11}	1.6	−0.9069	−0.1461	−0.3951	0.9987	0.0516	0.0007
σ_{22}	−64.3	0.0706	0.863143	−0.5000	− 0.059	0.9982	−0.0095
σ_{33}	−82.3	−0.4198	0.5466	0.7246	0.0175	− 0.0694	0.9974

	ppm	*x*	*y*	*Z*	DFT	ppm	*x*	*y*	*z*
HF									
σ_{11}	3.0	0.99842	0.05218	0.0209	σ_{11}	16.8	0.9991	−0.0357	−0.0213
σ_{22}	−56.4	−0.0323	0.9982	0.0509	σ_{22}	−74.6	0.0083	0.9962	0.0868
σ_{33}	−90.0	0.0045	0.0038	0.9999	σ_{33}	−90.4	−0.0083	0.0125	0.9999

Chemical shielding tensor values are referenced to TFA.
5- Fluoro-DL-tryptophan in D_2O, $\sigma_{iso} = -49.3$ ppm.

in Table 3. In the conventional single-crystal NMR method, in order to relate the direct cosines of the principal axis frame to the crystallographic frame, X-ray diffraction or optical goniometry is needed to determine the crystal holder orientations. This requires additional measurements and will inevitably introduce systematic errors. In this work, resolved F–F homonuclear dipole couplings in single-crystal NMR spectra provide us enough information to solve this problem. The theory has been introduced in Section 2. Fig. 5 shows the dipolar coupling splitting values plotted against rotation angles. By fitting these curves, the three Euler angles $(\alpha_X, \beta_X, \gamma_X)$ relating the crystal holder frame to the crystallographic frame were obtained. The values for these angles from the fit were $(\alpha_X, \beta_X, \gamma_X) = (-74.4°, 146.7°, 114.7°)$ and the best fits were shown in Fig. 5 by solid lines. The local molecular frame system, shown in Fig. 6, was defined as follows: the y axis lies parallel to the C–F bond, the z axis is perpendicular to the indole plane, and the x axis is the cross product of y and z. All the chemical shielding tensor elements and direction cosines comparing the principal axis frame to the local molecular frame were listed in Table 3. The orientation of the tensors is illustrated in Fig. 6. The principal values of the CSA tensor of 5F-Trp are defined in the conventional way $(\sigma_{11} \geqslant \sigma_{22} \geqslant \sigma_{33})$. They were determined from the averaged values of two chemically equivalent fluorine atoms; $\sigma_{11} = 0.9$, $\sigma_{22} = -63.3$, and $\sigma_{33} = -82.9$ ppm relative to

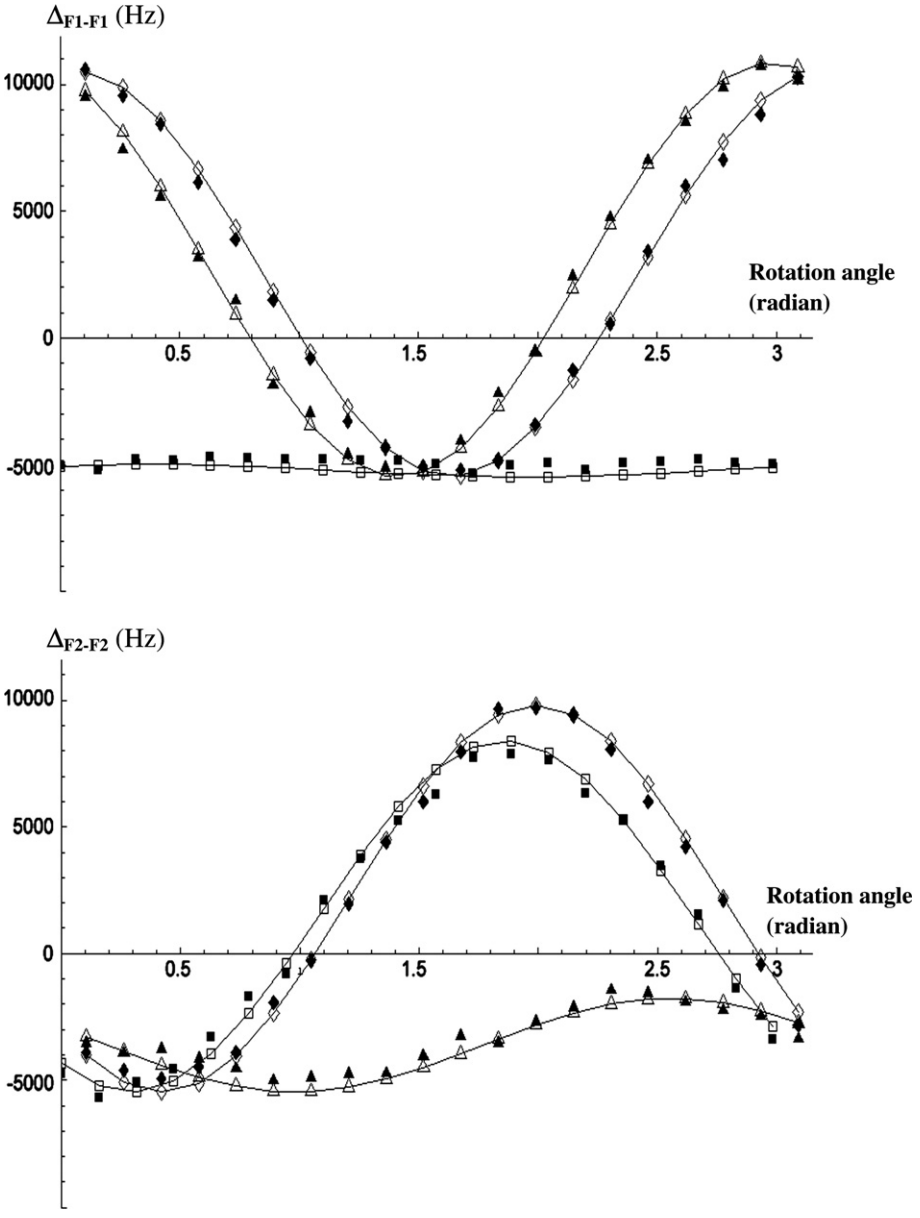

Fig. 5. All the ^{19}F NMR spectra in Fig. 3 are deconvolved with a pair of doublets and provide us with separated chemical shift and dipolar coupling values. These plots contain only dipolar coupling information. Two magnetically nonequivalent ^{19}F atoms were separated. In each plot different rotations are represented by different shapes. Rectangles are from x rotation, diamonds are from y rotation, and triangles are contributed by z rotation. Solid shapes are experimental values and hollow shapes connected by continuous lines are theoretical curves computed by the equations shown in Section 2 with best-fit Euler angles $(\alpha_X, \beta_X, \gamma_X)$ relating the crystal holder frame to the crystallographic frame.

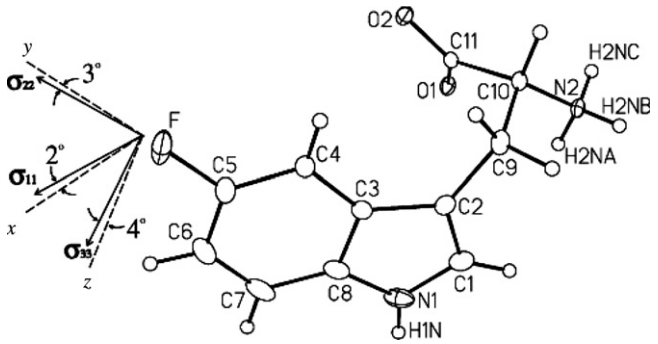

Fig. 6. Orientation of the principal axes labeled σ_{11}, σ_{22}, σ_{33} of the ^{19}F chemical shielding tensor in 5F-Trp as defined in the local molecular frame (x, y, z).

TFA at 0 ppm. The most shielded tensor component σ_{33} is generally perpendicular to the indole ring, with about a 4° deviation. σ_{22} lies approximately along the CF bond. The least shielded component σ_{11} is almost orthogonal to the CF bond in the indole ring plane; the respective deviations are 2° and 3°.

4. Discussion

The magnitudes of chemical shift shielding tensor elements determined for 5F-Trp are similar to those values found in mono-fluoro-benzene compounds [42]. Excluding the ''ortho-effect'', which is absent in 5F-Trp, the C–F bond length and molecular motions are the major factors in dictating tensor values. The p-orbital of the fluorine atom can strongly interact with the aromatic ring and has a significant impact on the local electric environment, especially along the C–F bond direction and the vector perpendicular to the aromatic ring. Theoretical calculation found a large shielding derivative (~460 ppm/Å) along the C–F bond [43]. Overall, our 5F-Trp data and other aromatic fluorine results [44–46] all suggest this character. Unlike the representative aromatic fluorine compound C_6F_6, which is rotating about its six-fold axis rapidly at room temperature [47,48] and yields an axially symmetric chemical shielding tensor [49], 5F-Trp molecules are effectively rigid in the ring plane so tensors σ_{11} and σ_{22} are not averaged by motion. A large asymmetric parameter (0.42) found in our results supports this conclusion. At high fields (564 MHz for ^{19}F in this work), chemical shift anisotropy is more important than ^{1}H–^{19}F dipole–dipole coupling in ^{19}F relaxation mechanisms. It was found that 5F-Trp has a long spin–lattice relaxation time ($T_1 = 234$ s), which also suggests a rigid local environment. However, whether or not it consists of 180° ring flips [50] can not be elucidated by chemical shift tensor data because the tensor itself is not influenced in this motion by symmetry. By using a Resolve-Al™ Gd doped sample, the T_1 can be shortened to 44 s.

There are two additional verifications which can be applied to the single-crystal NMR data in Table 3. First of all, we can compare the results with other methods. There is some disagreement between these values and those obtained earlier in our group from a static powder NMR spectrum [30] probably because strong F–F dipolar coupling contributions in the ^{19}F NMR powder pattern were overlooked in the previous study. Grage et al. [51] measured ^{19}F chemical shift shielding tensor values in 5F-Trp labeled gramicidin A from powder spectra at 5 °C. The values they obtained, ($\sigma_{11} = -2.0, \sigma_{22} = -65.5, \sigma_{33} = -80.5$ ppm, referenced to TFA), are quite close to our single-crystal results. Because 5F-Trps are isolated in the peptide sample, F–F dipolar couplings become negligible. In addition, $\sigma_{iso} = \frac{1}{3}(\sigma_{11} + \sigma_{22} + \sigma_{33})$, so the ^{19}F isotropic chemical shift from the liquid-state can also serve as a check on the single-crystal data; The result is in good agreement with the single-crystal data in Table 3.

Ab initio quantum chemical and DFT methods are also available to investigate chemical shielding in both simple and complex systems [52,53]. Therefore, it is interesting to compare the experimental tensor values and principal axes with those obtained by theoretical calculations. Since the time-consuming MP2-GIAO method does not provide obvious improvements in fluorobenzene calculations [43], HF-GIAO and DFT-GIAO methods were used in this work. The results are listed in Table 3. In both cases, the magnitudes of the computed chemical shielding tensor elements are moderately close to experimental values. DFT calculations did a better job in their relative magnitudes possibly because of the electron correlations between the fluorine atom p-orbital and aromatic ring. It is known that the results from the calculations correspond to the isolated molecule in the gas phase, so generally the calculated values are overestimated, as shown in Table 3. By considering the dielectric effect and applying vibrational averages to these calculations, the discrepancy may be marginally reduced. The agreement between experimental chemical shielding tensor directions and those from the calculations is gratifyingly good. Single-crystal NMR studies and the theoretical calculations produced deviations of 1° to 3° from the local frame axes. In both cases, these deviations are too small to be identified as real results or systematic errors. Overall, the theoretical calculations positively support the results obtained in single-crystal NMR.

This study provides a solid experimental basis for a ^{19}F NMR strategy using 5F-Trp labeled proteins to investigate biomacromolcular orientation at the *in situ* level.

Acknowledgments

Dr. Gerard S. Harbison at the University of Nebraska-Lincoln is thanked for useful discussion about data processing strategies. We thank the Alberta Heritage Foundation for Medical Research for postdoctoral fellowship support (Xingang Zhao) and financial support by Canada Research Chairs and Canadian Institutes of Health Research. We thank Sam Graziano at the University of Alberta for machining the goniometer portion of the probe.

References

[1] M. Bjerring, T. Vosegaard, A. Malmendal, N.C. Nielsen, Concept. Magn. Reson. A 18A (2) (2003) 111–129.
[2] S.J. Opella, Nat. Struct. Biol. 4 (Suppl) (1997) 845–848.
[3] A. Watts, Biochimica et Biophysica Acta, Rev. Biomembr. 1376 (3) (1998) 297–318.
[4] R. Tycko, Annu. Rev. Phys. Chem. 52 (2001) 575–606.
[5] D. O'Hagan, D.B. Harper, J. Fluor. Chem. 100 (1999) 127–133.
[6] W.E. Hull, B.D. Sykes, Biochemistry 13 (1974) 3431–3437.
[7] W.E. Hull, B.D. Sykes, J. Mol. Biol. 98 (1975) 121–153.
[8] W.E. Hull, B.D. Sykes, Biochemistry 15 (1976) 1535–1546.
[9] F. Sixl, R.W. King, M. Bracken, J. Feeney, Biochem. J. 266 (1990) 545–552.
[10] A.S. Ulrich, Prog. Nucl. Magn. Reson. Spectrosc. 46 (2005) 1–21.
[11] http://www.nhlbi.nih.gov/health/hearttruth/whatis/index.htm.
[12] D.A. Lindhout, B.D. Sykes, J. Biol. Chem. 278 (29) (2003) 27024–27034.
[13] M.X. Li, X. Wang, B.D. Sykes, J. Muscle Res. Cell Motil. 25 (7) (2004) 559–579.
[14] B.D. Sykes, Nat. Struct. Biol. 10 (8) (2003) 588–589.
[15] X. Wang, P. Mercier, P. Letourneau, B.D. Sykes, Prot. Sci. 14 (2005) 2447–2460.
[16] R.R. Ketchem, B. Roux, T.A. Cross, Structure 5 (1997) 1655–1669.
[17] R.E. Koeppe II, J.A. Killian, D.V. Greathouse, Biophys. J. 66 (1994) 14–24.
[18] M. Cotton, F. Xu, T.A. Cross, Biophys. J. 73 (1997) 614–623.
[19] S.F. Scarlata, Biophys. J. 54 (1988) 1149–1157.
[20] S.F. Scarlata, Biochemistry 30 (1991) 9853–9859.
[21] T. Maruyama, H. Takeuchi, Biospectroscopy 4 (1998) 171–184.
[22] A.M. Weljie, H.J. Vogel, Protein Eng. 13 (2000) 59–66.
[23] L. McDowell, M. Lee, R.A. McKay, K.S. Anderson, J. Schaefer, Biochemistry 35 (1996) 3328–3334.
[24] J.T. Gerig, Prog. NMR Spec. 26 (1994) 293–370.
[25] M. Bouchard, C. Pare, J.P. Dutasta, J.P. Chauvet, C. Gicquaud, M. Auger, Biochemistry 37 (1998) 3149–3155.
[26] T. Vosegaard, V. Langer, P. Daugaard, E. Hald, H. Bildsoe, H.J. Jakobsen, Rev. Sci. Instrum. 67 (6) (1996) 2130–2133.
[27] H. Hauser, C. Radloff, R.R. Ernst, S. Sundell, I. Pascher, J. Am. Chem. Soc. 110 (1988) 1054–1058.
[28] G.M. Sheldrick, Acta Crystallogr. A46 (1990) 467–473.
[29] G.M. Sheldrick, SHELXL-93. Program for Crystal Structure Determination, University of Göttingen, Germany, 1993.
[30] S.P. Graether, J.S. DeVries, R. McDonald, M.L. Rakovszky, B.D. Sykes, J. Magn. Reson. 177 (2005) 433–439.
[31] J.M. Miller, Prog. NMR Spectrosc. 28 (1996) 255–281.
[32] Gaussian 03, Revision A. l, M.J. Frisch, G.W. Trucks, H.B. Schlegel, G.E. Scuseria, M.A. Robb, J.R. Cheeseman, J.A. Montgomery, Jr. T. Vreven, K.N. Kudin, J.C. Burant, J.M. Millam, S.S. Iyengar, J. Tomasi, V. Barone, B. Mennucci, M. Cossi, G. Scalmani, N. Rega, G.A. Petersson, H. Nakatsuji, M. Hada, M. Ehara, K. Toyota, R. Fukuda, J. Hasegawa, M. Ishida, T. Nakajima, Y. Honda, O. Kitao, H. Nakai, M. Klene, X. Li, J.E. Knox, H.P. Hratchian, J.B. Cross, C. Adamo, J. Jaramillo, R. Gomperts, R.E. Stratmann, O. Yazyev, A.J. Austin, R. Cammi, C. Pomelli, J.W. Ochterski, P.Y. Ayala, K. Morokuma, G.A. Voth, P. Salvador, J.J. Dannenberg, V.G. Zakrzewski, S. Dapprich, A.D. Daniels, M.C. Strain, O. Farkas, D.K. Malick, A.D. Rabuck, K. Raghavachari, J.B. Foresman, J.V. Ortiz, Q. Cui, A.G. Baboul, S. Clifford, J. Cioslowski, B.B. Stefanov, G. Liu, A. Liashenko, P. Piskorz, I. Komaromi, R.L. Martin, D.J. Fox, T. Keith, M.A. Al-Laham, C.Y. Peng, A. Nanayakkara, M. Challacombe, P.M.W. Gill, B. Johnson, W. Chen, M.W. Wong, C. Gonzalez, A. Pople, Gaussian Inc., Pittsburgh PA, 2003.
[33] A.D. Becke, J. Chem. Phys. 98 (1993) 5648–5652.
[34] C.T. Lee, W.T. Yang, R.G. Parr, Phys. Rev. B 37 (1988) 785–789.
[35] W.J. Hehre, L. Radom, P.V.R. Schleyer, J.A. Pople, Ab Initio Molecular Orbital Theory, John Wiley, New York, 1986.
[36] F.J. London, Phys. Radium 8 (1937) 3974–3976.
[37] R. Ditchfield, Mol. Phys. 27 (1974) 789–807.
[38] K. Wolinski, J.F. Himton, P. Pulay, J. Am. Chem. Soc. 112 (1990) 8251–8260.
[39] W. Luo, M. Hong, J. Am. Chem. Soc. 128 (2006) 7242–7251.
[40] Ch. B. Hubschle, M. Messerschmidt, P. Luger, Cryst. Res. Technol. 39 (2004) 274–278.
[41] M.A. Kennedy, P.D. Ellis, Concept Magnetic Res. 1 (1989) 35–47, 109-129.
[42] H. Raber, M. Mehring, Chem. Phys. 26 (1977) 123–130.
[43] L.K. Sanders, E. Oldfield, J. Phys. Chem. A 105 (2001) 8098–8104.
[44] R.G. Griffin, H.-N. Yeung, M.D. LaPrade, J.S. Waugh, J. Chem. Phys. 59 (1973) 777–783.
[45] Y. Hiyama, J.V. Silverton, D.A. Torchia, J.T. Gerig, S.J. Hammond, J. Am. Chem. Soc. 108 (1986) 2715–2723.
[46] E.E. Burnell, A.L. Mackay, D.C. Roe, A.G. Marshall, J. Magn. Reson. 45 (1981) 344–351.
[47] J.S. Waugh, E.I. Fedin, Soviet Phys. Solid State 4 (1963) 1633.
[48] E.R. Andrew, J. Chem. Phys. 18 (1950) 607.
[49] M. Mehring, R.G. Griffin, J.S. Waugh, J. Chem. Phys. 55 (1971) 746–755.
[50] J.A. Ripmeester, R.K. Boyd, J. Chem. Phys. 71 (1979) 5167.
[51] S.L. Grage, J. Wang, T.A. Cross, A.S. Ulrich, Biophys. J. 83 (2002) 3335–3336.
[52] A.C. de Dios, E. Oldfield, J. Am. Chem. Soc. 116 (1994) 7453–7454.
[53] W.D. Arnold, J. Mao, H. Sun, E. Oldfield, J. Am. Chem. Soc. 122 (2000) 12164–12168.